



45th SME North American Manufacturing Research Conference, NAMRC 45, LA, USA

## Investigation on grindability of medical implant material using a silicon carbide wheel with different cooling conditions

P.Suya Prem Anand<sup>a\*</sup> N.Arunachalam<sup>b</sup> and L.Vijayaraghavan<sup>c</sup>

<sup>a</sup>Research Scholar, Department of Mechanical Engineering, Indian Institute of Technology Madras, Chennai, India

<sup>b</sup>Assistant Professor, Department of Mechanical Engineering, Indian Institute of Technology Madras, Chennai, India

<sup>c</sup>Professor, Department of Mechanical Engineering, Indian Institute of Technology Madras, Chennai, India

<sup>a</sup>[suyaprime@yahoo.co.in](mailto:suyaprime@yahoo.co.in), <sup>b</sup>[chalam@iitm.ac.in](mailto:chalam@iitm.ac.in), <sup>c</sup>[lvijay@iitm.ac.in](mailto:lvijay@iitm.ac.in)

### Abstract

Zirconia is the preferred material used in many applications including biomedical implant. The zirconia in its sintered form is the most preferred one to manufacture a near net shaped implant material with minimal work. But it is very difficult to shape as the material chip away during the machining or grinding process. Hence zirconia in a pre-sintered form is used to achieve the required shape and size for a specific application. Then it is sintered and used. In this work, the grindability of the pre-sintered zirconia was evaluated using a dense vitreous bond silicon carbide wheel. The grinding parameters such as wheel speed, radial depth of cut and feed rate are varied to investigate its grindability in terms of force ratio, specific energy, surface finish, G-ratio and ground surface under both wet and MQL cooling conditions. The forces produced during the grinding of pre-sintered zirconia was observed lower in the MQL (Minimum Quantity Lubrication) technique due to the reduction of friction, when compared to the wet cooling condition. The calculated specific energy was less in MQL cooling condition, due to the reduction in heat generation and friction. The surface finish of the workpiece obtained from the wet cooling condition was better due to the reduction in wheel loading. The percentage difference of the G-ratio between both the wet and MQL cooling conditions was observed to be 24 percent. This was due to the active participation of grains and less wheel loading in wet grinding condition. The ground surfaces obtained from the wet cooling condition were smooth and regular, compared to the MQL grinding condition.

*Keywords:* Force Ratio; Wheel Wear; Surface Finish; Grinding Fluid

### 1. Introduction

Recently zirconia based ceramics are used in the medical implants due to their advanced mechanical properties like high fracture toughness compared to other alternatives, which provides resistance to crack formation during the grinding process. The various compounds such as magnesium oxides, yttrium oxides and cerium oxides are added to pure zirconia to retain the tetragonal phase at room temperature and to enhance the properties of the

material. Yttria stabilized tetragonal zirconia (Y-TZP) is predominantly used as the base material for manufacturing dental crown, hip joints and fixed dentures of biomedical application [1]. Both the pre-sintered and fully sintered blocks are frequently used in this fabrication process, where porous components are easy to machine due to their soft nature as compared to the sintered zirconia. As the pre-sintered block has lesser hardness, when compared to the sintered zirconia, it improves the machinability of the sample without the formation of chipping. Pre-Sintered zirconia is used in dentistry for making dental crowns and fixed partial dentures. The components are machined in the pre-sintered block prior to sintering at high temperature or in fully sintered blocks. Machining of sintered block is extremely difficult because of its densely packed grains, high hardness and low machinability [2,3].

The fine grit abrasive of silicon carbide paper is used to finish the pre-sintered block to the required tolerance limit and surface finish [4]. The experiments were conducted under the wet cooling condition to analyze the grindability of silicon carbide wheel on different forms of zirconia. The grindability of ceria added zirconia is studied by using different types of grinding wheel, such as diamond, CBN and silicon carbide grinding wheels. The grinding forces, specific energy and surface finish are estimated and the results showed that the silicon carbide wheel is used effectively to grind zirconia [5]. Silicon carbide wheel of grit size 220 with low porosity vitreous bonds is used to grind the zirconia, because it reduces the necessity of dressing by producing the least amount of wheel wear while grinding zirconia. Also the cost of SiC wheel is cheaper than using the diamond grinding wheel [6].

During grinding of both fully and partially stabilized zirconia using a fine grain vitreous bond silicon carbide wheel, the phase transformation analysis is performed on the chips and the ground surfaces using the X-ray diffractometer. The result shows a decrease in the thermal conductivity of zirconia chips and silicon carbide grinding wheel, which supports the softer material removal and reduces the wheel wear [7]. The fine grain dense vitreous bond silicon carbide wheel can be used to grind silicon nitride ceramics, where the grinding force and the wheel wear are increased to a higher level during the grinding process. It supports the precision form of grinding, which improves the G-ratio and surface integrity of the workpiece. When the radial depth of cut and material removal rate increases, it leads to higher wheel wear [8].

Another problem associated with the wet grinding of zirconia is the phase transformation, which takes place due to the difference in temperature and the hydrothermal loading that occurs during the grinding process. When yttrium stabilized tetragonal zirconia is subjected to a moisture environment, it increases the percentage of the monoclinic phase, which is the weakest form of phase among all the three phases in zirconia. Although the tetragonal phase helps in favor of resisting the external stress by increasing the fracture toughness, the strength degradation takes place due to the changes in the microstructure of the material such as microcracks, voids and grain growth [9]. To investigate the impact of portable grinding on Y-TZP (Yttria stabilized tetragonal zirconia) in terms of phase transformation, ground surface and aging process, the experiments are carried out in water cooling condition with various grit sizes. The percentage of the monoclinic phase increases due to the effect of grinding and the aging process, which affects the mechanical properties of the material [10]. The Zirconia (Y-TZP) material is subjected to a hydrothermal loading by varying the temperature and the time. Raman spectroscopic analysis is performed on the samples to detect the depth of the transformation zone. Due to this coolant assisted heating, the phase transformation takes place on the surface and extends to a certain depth. When the samples are tested by Vicker hardness test, the hardness value decreases with the depth of transformation zone [11].

The MQL is used to deliver a minimum quantity of fluid at the contact zone and concentrate more on lubrication by reducing the friction rather than cooling the surfaces. The lubricant applied in the contact zone reduces the friction and minimizes the thermal damages caused by grinding. Minimizing the amount of coolant in the grinding process leads to the reduction of environmental effects and cost. The surface finish improves in the MQL technique by supplying a small amount of fluid at the contact zone. When the MQL technique is compared with the wet grinding process, the grinding force, surface roughness and surface damages are reduced and the surface quality is improved in the MQL grinding process, as the cutting fluid in the wet grinding process does not fully penetrate into the grinding contact zone [12]. The MQL technique is used along with cleaning compressed air to replace the wet coolant process in cylindrical grinding of tempered and quenched steel. When using the minimum quantity of fluid, it provides insufficient cooling and the chips are not completely washed away by the fluid, which brings harmful effect to the surface of the workpiece and increases the heat generation. The output variables such as wheel wear, roundness error and workpiece surface roughness are analyzed, which shows a improvement in MQL fluid flow by implementing a jet of compressed air at different angles for cleaning the wheel surface [13]. The impact of

using MQL fluid on the grinding of sintered zirconia ceramic with resin bond diamond wheel is studied by considering the grinding force, surface roughness and sub surface damages. The performance is compared to the wet coolant condition, but the result obtained from the MQL cooling condition shows a better surface finish, low grinding force and less damage [14].

In order to evaluate the wheel wear of silicon carbide wheel on grinding of pre-sintered zirconia during the grinding process, the MQL lubrication technique was used to analyze the cooling effect of oil on grinding zirconia and to improve the *G-ratio* of silicon carbide wheel. However, MQL technique depends on the type of material, grinding wheel and the form of chip produced from the grinding process, where two kinds of scenarios are possible, such as 1) If the grinding wheel consists of multiple pores, the powdered chips will fill the pores and will come into repeated contact with the surface and deteriorate the surface finish of the material, 2) If the supplied coolant is not sufficient to remove the chips from the grinding wheel, it will result in wheel loading. The grindability of pre-sintered zirconia was investigated with SiC wheel under both wet and MQL cooling conditions based on the force ratio, specific energy, surface finish, G-ratio and ground surface topography.

## 2. Experimental Work

The experiments were designed based on the central composite design. It had been essential to use central composite design to reduce the number of experiments to 20. It consisted of three points like factorial, axial and central points, where the eight edge point (-1.68 & 1.68) represented the design limits, the six axial points (-1 & 1) were some distance away from the centre depending on the number of factors and the six centre points (0) completed the design. The levels and factors selected for the experiments are given in the Table 1. Pre-Sintered zirconia was used as the work piece material in this experiment and the grain size was varied from 0.15 to 0.35  $\mu\text{m}$ . The mechanical properties of the pre-sintered zirconia are listed in Table 2. The density and hardness of sintered zirconia vary from the porous material such as 6080  $\text{Kg/m}^3$  and 1250 Hv.

Table 1. Design of grinding factors and their levels

| S.No | Grinding Parameters                          | Factor Levels (Limits) |    |    |    |      |
|------|--|------------------------|----|----|----|------|
|      |  | -1.68                  | -1 | 0  | 1  | 1.68 |
| 1    | Wheel Speed, $V_s$ (m/s)                     | 22                     | 26 | 32 | 36 | 42   |
| 2    | Radial Depth of Cut, $a_c$ ( $\mu\text{m}$ ) | 10                     | 15 | 20 | 25 | 30   |
| 3    | Feed Rate, $V_f$ (m/min)                     | 2                      | 4  | 6  | 8  | 10   |

Table 2. Mechanical properties of pre-sintered zirconia

| S.No | Density ( $\text{Kg/m}^3$ ) | Flexural Strength (MPa) | Hardness Hv | Young's Modulus (GPa) | Fracture Toughness ( $\text{MPa m}^{1/2}$ ) |
|------|-----------------------------|-------------------------|-------------|-----------------------|---|
| 1    | 3030                        | > 1000                  | 64          | 210                   | 8.05  |

A fine grit vitreous bond silicon carbide wheel of specification GC120 H6 VPF was used as the grinding wheel with a dimension of 200 mm diameter and 12.7 mm wheel width. The grinding parameters such as wheel speed, radial depth of cut and feed rate were varied to analyze the performance of silicon carbide wheel on pre-sintered zirconia. The grinding conditions used for the experiments are given in Table 3.

Table 3. Grinding Conditions

| S.No | Grinding Conditions       | Specification  |
|------|---------------------------|--|
| 1    | Wheel Speed $V_s$         | 22, 26, 32, 36 and 42 (m/s)                                  |
| 2    | Radial Depth of Cut $a_e$ | 10, 15, 20, 25 and 30 ( $\mu\text{m}$ )                      |
| 3    | Feed Rate $V_f$           | 2, 4, 6, 8 and 10 (m/min)                                    |
| 4    | Grinding Wheel            | GC120 H6 VPF   |
| 5    | Work Piece Material       | (Y-TZP) Grain Size 0.15 to 0.35 $\mu\text{m}$<br>65×30×20 mm |
| 6    | Type of Grinding          | Peripheral Grinding  |
| 7    | MQL Fluid                 | Synthetic oil  |
| 8    | Coolant                   | Water soluble oil (5% concentration)                         |
| 9    | Fluid Flow Rate           | 250 ml/hr (MQL)<br>80 l/hr (Wet Coolant)                     |
| 10   | Air Pressure              | 6 bar  |

The experiments were conducted on a peripheral surface grinding machine (chevalier H-B81-8II) and the grinding forces were measured using a dynamometer (Kistler 9257 B type). A machine vision system with CCD camera having a resolution of 1024×1024 pixels was used to acquire images of wheel surface after each grinding experiment, where a lens with a magnification of 20 X was used in this experiment. A single point diamond dresser was used to dress the silicon carbide wheel for each grinding cycle, where 10  $\mu\text{m}$  had been used as the dressing radial depth of cut and 100 mm/min was used as the cross feed velocity of the dresser. The dressing lead was 32  $\mu\text{m}$  calculated from the wheel velocity and the velocity of the dresser. The experimental setup has been depicted in Fig 1. An MQL setup was equipped with a control system which consist of a peristaltic pump to adjust the fluid flow rate of 250 ml/hr and the air was supplied at a pressure of 6 bar from the compressor and connected to the atomizing nozzle. The other end of the nozzle was connected to the fluid supply from the reservoir, where synthetic oil was used as a MQL lubricant. The nozzle was placed at a distance of 80 mm away from the center of the wheel and height 15 mm from the bottom of the wheel. In wet cooling condition, water soluble oil was used as the cutting fluid with a concentration of 5 percentage. A pliable nozzle was used to supply the fluid at a pressure of 1 bar and a flow rate of 80 l/hr.

The grinding power  $P$  was calculated using the measured tangential grinding force  $F_t$  (N) and the wheel speed  $V_s$  (m/s)

$$P = F_t V_s \quad (1)$$

The specific energy  $U$  ( $\text{J}/\text{mm}^3$ ) and volumetric removal rate  $Q_w$  ( $\text{mm}^3/\text{s}$ ) were calculated using the equations.

$$U = P/Q_w \quad (2)$$

$$Q_w = V_w a_e b \quad (3)$$

Where  $V_w$ ,  $a_e$  and  $b$  are the feed rate (m/min), radial depth of cut ( $\mu\text{m}$ ) and wheel width (m)

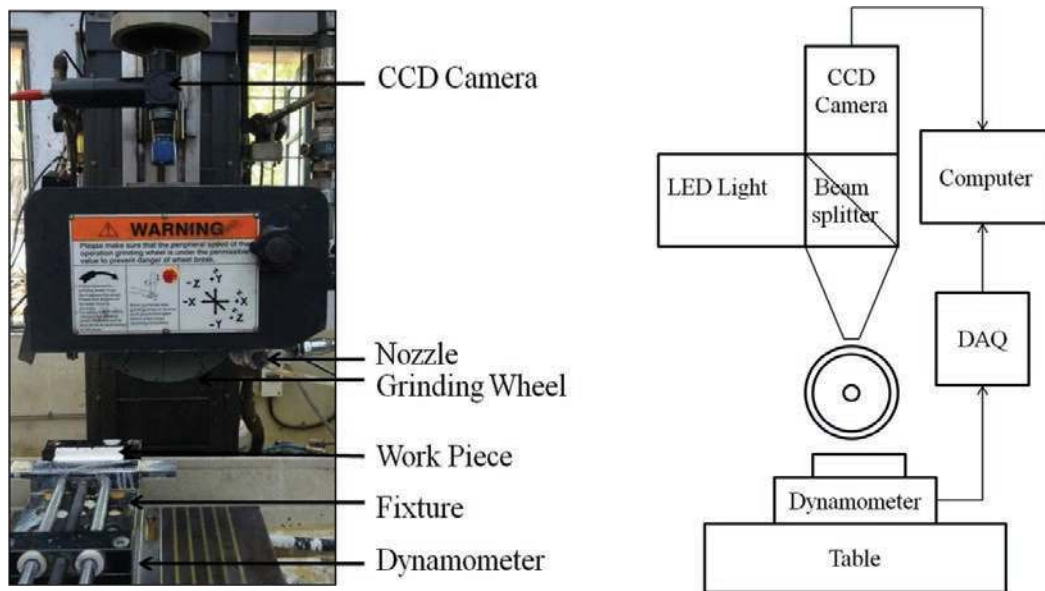


Fig. 1. Photograph and schematic diagram of experimental setup

The forces were measured for every ten grinding passes and the grinding wheel was dressed for each cycle. A 3-D non contact (Bruker) surface profiler was used to measure the average surface roughness  $R_a$  of the ground samples. Totally four measurements were taken across the grinding direction and an area of  $640 \times 480 \mu\text{m}$  was covered. The surface morphology was analyzed with the help of SEM (Scanning Electron Microscope) images. To analyze the wheel wear of silicon carbide wheel under both wet and MQL cooling conditions, grinding experiments were carried out separately on a continuous basis without dressing the grinding wheel for about 280 passes. The grinding condition used was same for both the conditions with a 32 m/s grinding speed, 20  $\mu\text{m}$  radial depths of cut and 6 m/min feed rate. The weight of the grinding wheel and sample was measured before and after the grinding process to calculate the volume of material removed from both the work piece and the grinding wheel.

### 3. Results and Discussion

#### 3.1 Force ratio

The force ratio variation was observed under different wheel speed and radial depth of cut for both the wet and MQL conditions. The observed force ratio mainly depends on the cutting action of the grain rather than the rubbing and ploughing operations. The force ratio during the wet grinding process was lower for lesser wheel speed due to the increase in the actual contact area and the active participation of grains in the grinding process as shown in Fig 2 (a). Overall, the force ratio observed was higher for the MQL cooling condition. This could be due to the occurrence of wheel loading and the inter layer formation between the wheel and the work piece surface. The powdered chip particles were filled in the pores of the grinding wheel due to the supply of low volume pressurized oil mist. As the radial depth of cut increased in wet grinding condition, the force ratio raised initially and stabilized, which showed that the rate of material removal was lesser for higher radial depth of cut as shown in Fig 2 (b). This could be due to the effect of heat dissipation and the rise in tangential force during the wet grinding process. This increase in temperature caused the bond to degrade severely, which resulted in distortion and reduced the grit retention in the wheel.

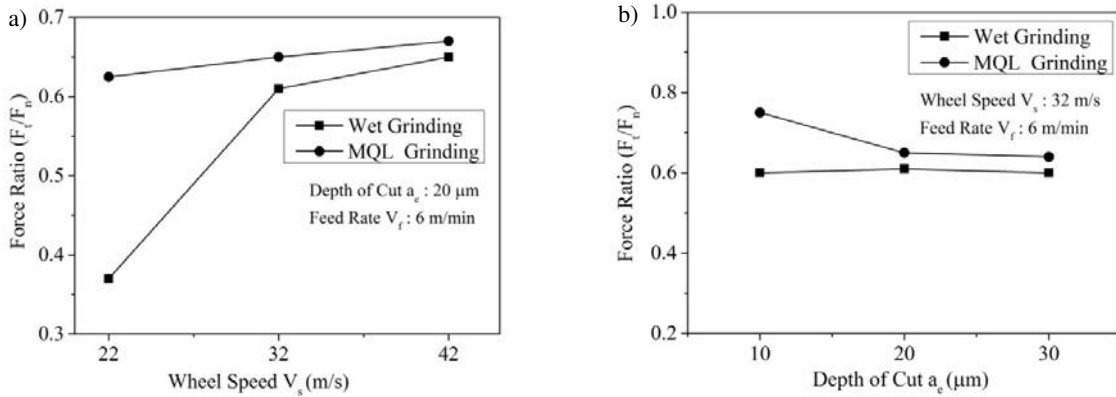


Fig. 2. (a) Effect of wheel speed on force ratio, (b) Effect of radial depth of cut on force ratio

In addition, the force ratio produced at a 10 $\mu\text{m}$  radial depth of cut was high during the MQL grinding condition. Thereafter, it reduced drastically, which may be due to the rubbing and the ploughing operation of the grinding wheel. The grinding forces, specific energy and surface roughness for both the wet and MQL grinding conditions are listed in Table 4.

Table 4. Grinding forces, specific energy and surface roughness

| S.N<br>o | Grinding parameters      |  |                          | Wet Grinding Condition      |                         |   |  | MQL Grinding Condition      |                         |   |  |
|----------|--------------------------|--|--------------------------|-----------------------------|-------------------------|---|--|-----------------------------|-------------------------|---|--|
|          | Wheel Speed, $V_s$ (m/s) | Radial Depth of Cut, $a_e$ ( $\mu\text{m}$ ) | Feed Rate, $V_f$ (m/min) | Tangential Force, $F_t$ (N) | Normal Force, $F_n$ (N) | Specific Energy, $U$ ( $\text{J}/\text{mm}^3$ ) | Surface Roughness, $R_a$ ( $\mu\text{m}$ ) | Tangential Force, $F_t$ (N) | Normal Force, $F_n$ (N) | Specific Energy, $U$ ( $\text{J}/\text{mm}^3$ ) | Surface Roughness, $R_a$ ( $\mu\text{m}$ ) |
| 1        | 22                       | 20   | 6                        | 3.2                         | 8.5                     | 2.64  | 0.63                                       | 2.5                         | 4                       | 2.05  | 2.18                                       |
| 2        | 32                       | 20   | 6                        | 1.7                         | 2.8                     | 2.10  | 0.615                                      | 1.3                         | 2                       | 1.61  | 1.64                                       |
| 3        | 42                       | 20   | 6                        | 1.5                         | 2.3                     | 2.47  | 0.519                                      | 1.2                         | 1.8                     | 1.98  | 0.978                                      |
| 4        | 32                       | 10   | 6                        | 1.2                         | 2                       | 2.96  | 0.585                                      | 0.6                         | 0.8                     | 1.48  | 1.1  |
| 5        | 32                       | 30   | 6                        | 2.5                         | 4.2                     | 2.06  | 0.715                                      | 2.2                         | 3.4                     | 1.81  | 1.62                                       |
| 6        | 26                       | 15   | 4                        | 1.3                         | 2.6                     | 2.67  | 0.723                                      | 1.1                         | 1.6                     | 2.26  | 1.13                                       |
| 7        | 36                       | 15   | 4                        | 0.8                         | 1.2                     | 2.30  | 0.739                                      | 0.5                         | 1                       | 1.44  | 0.776                                      |
| 8        | 26                       | 25   | 4                        | 2.2                         | 5.3                     | 2.71  | 0.891                                      | 1.8                         | 2.4                     | 2.22  | 2.35                                       |
| 9        | 36                       | 25   | 4                        | 1.5                         | 2.3                     | 2.60  | 0.783                                      | 1.2                         | 2.3                     | 2.07  | 1.44                                       |
| 10       | 26                       | 15   | 8                        | 1.6                         | 3.5                     | 1.65  | 0.939                                      | 1.4                         | 2.1                     | 1.44  | 1.72                                       |
| 11       | 36                       | 15   | 8                        | 1.5                         | 3.2                     | 2.16  | 0.762                                      | 1.3                         | 1.8                     | 1.87  | 1.18                                       |
| 12       | 26                       | 25   | 8                        | 2.5                         | 4.2                     | 1.54  | 0.923                                      | 2.4                         | 4                       | 1.48  | 1.8  |
| 13       | 36                       | 25   | 8                        | 2                           | 3.6                     | 1.73  | 0.905                                      | 2.1                         | 2.8                     | 1.82  | 1.68                                       |
| 14       | 32                       | 20   | 2                        | 1.3                         | 2.3                     | 4.82  | 1.11                                       | 1.2                         | 1.8                     | 4.45  | 1.51                                       |
| 15       | 32                       | 20   | 10                       | 2.2                         | 4.2                     | 1.63  | 0.756                                      | 2                           | 3                       | 1.48  | 1.8  |
| 16       | 32                       | 20   | 6                        | 1.6                         | 2.8                     | 1.97  | 0.620                                      | 1.4                         | 2.2                     | 1.73  | 1.68                                       |
| 17       | 32                       | 20   | 6                        | 1.7                         | 2.7                     | 2.10  | 0.618                                      | 1.3                         | 2.1                     | 1.59  | 1.62                                       |

|    |    |    |   |     |     |      |       |     |     |      |      |
|----|----|----|---|-----|-----|------|-------|-----|-----|------|------|
| 18 | 32 | 20 | 6 | 1.8 | 2.7 | 2.23 | 0.616 | 1.5 | 2.2 | 1.85 | 1.63 |
| 19 | 32 | 20 | 6 | 1.7 | 2.8 | 2.10 | 0.619 | 1.4 | 2.0 | 1.73 | 1.70 |
| 20 | 32 | 20 | 6 | 1.7 | 2.9 | 2.10 | 0.615 | 1.3 | 2.2 | 1.59 | 1.64 |

### 3.2 Variations of specific energy with respect to material removal rate

Normally the specific energy decreases with increase in the material removal rate and the specific energy captures the work done to remove the material from the work piece. In the wet grinding process, the specific energy facilitated to remove the material easily with minimum work. There was a viscous, sticky inter layer formation observed between the grinding wheel and the work piece surface in MQL grinding condition, which might lead to ineffective grinding. The material removal in MQL process became much more complicated due to the viscosity of the fluid, which formed a colloidal paste on the surface of the grinding wheel and resulted in rubbing and ploughing operation. In the wet grinding process, the absence of interlayer formation caused the effective cutting edges to actively participate and the wet coolant tried to wash away the chip particles present in the pores of the grinding wheel. The gradual decrease of specific energy was obtained from the wet cooling condition, where the energy required for the maximum radial depth of cut reduced due to the increase in material removal rate as shown in Fig 3. The specific energy observed in the MQL condition was lowered, when compared to the wet cooling condition due to the reduction in heat generation and friction at the contact zone. However, the specific energy of MQL condition increased to a higher value for maximum speed because of the influence of more rubbing action that took place in the grinding process.

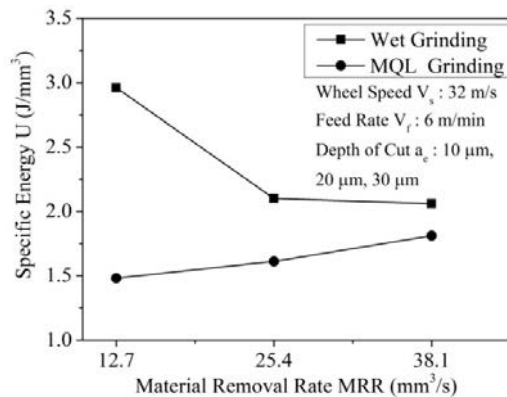


Fig. 3. Effect of material removal rate on specific energy

### 3.3 Surface Roughness

The wheel speed and radial depth of cut were varied to obtain the changes in surface roughness of both wet and MQL cooling conditions. The surface roughness obtained from the wet cooling condition showed a better finish compared to the MQL cooling condition, due to the proper supply of the coolant, which washed away the chips from the grinding zone. The magnitude of surface roughness was low, even at higher depths of cut due to the active participation of the grains in the wet grinding process. In case of MQL grinding, there was a rise in the roughness value at 20  $\mu\text{m}$  radial depth of cut. Thereafter the roughness remained constant with an increase in the radial depth of cut. The observed surface roughness was more in the MQL grinding process due to the wheel loading, which was caused by the viscosity of the oil. This might not allow the fluid to flow in between the grains and remove the chip particles in the grinding wheel. The variation of surface roughness with respect to wheel speed and radial depth of cut is shown in Fig 4 (a) & (b).

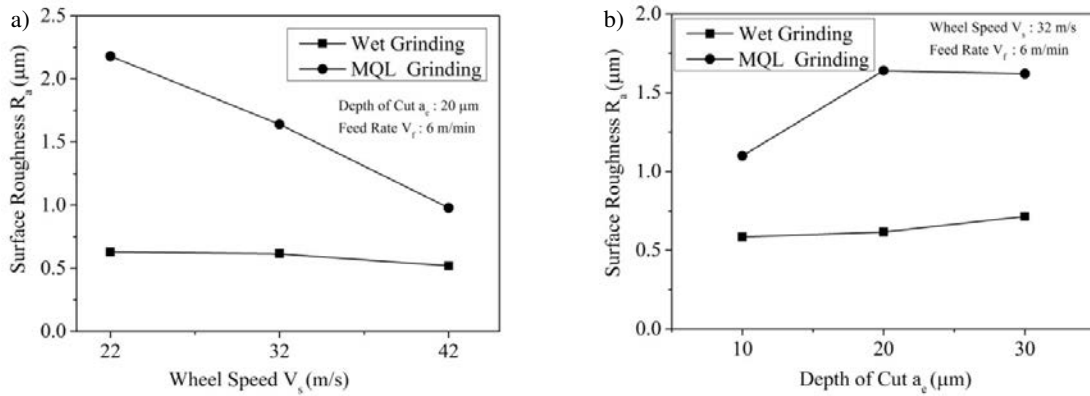


Fig. 4. (a) Effect of wheel speed on surface roughness, (b) Effect of radial depth of cut on surface roughness

### 3.4 Wheel Wear

During the analysis of the G-ratio of the SiC grinding wheel under both the wet and MQL condition, the obtained grinding forces showed a gradual increase for every 20 passes and reached a higher value. Thereafter, it reduced a little and got stabilized for the remaining passes, which confirmed that the wheel got worn out completely in wet grinding condition because of the active interaction of the grains. The forces observed for number of passes increased in MQL cooling condition compared to the wet cooling condition due to the interlayer formation and the presence of wheel loading. Therefore, the grains were not properly engaged in cutting action for the MQL cooling condition. The variations of normal force and tangential force with respect to the number of grinding passes are shown in Fig 5 (a) & (b).

The G-ratio was calculated from the equation as

$$G = \Delta V_w / \Delta V_s \tag{4}$$

Where  $\Delta V_w$  was the volume of material removed from the work piece and  $\Delta V_s$  was the volume of wheel wear. The estimation of G-ratio for silicon carbide wheel is listed in Table 5. The G-ratio of silicon carbide wheel increased under the wet cooling condition with more wheel wear, which reduced the life of the grinding wheel as shown in Fig 6 (b). This also assured that the material removal rate was higher in wet cooling condition. As the grains were not involved in cutting action under MQL cooling condition, the possibility of wheel wear was reduced in this cooling condition as shown in Fig 6 (d). This confirms that the material removal was less in the MQL cooling condition.

Table 5: Estimation of G-ratio for silicon carbide wheel

| S.NO | Cooling Conditions | Volume of material removed $\Delta V_w$ ( $\text{cm}^3$ ) | Volume of wheel wear $\Delta V_s$ ( $\text{cm}^3$ ) | G-ratio |
|------|--------------------|---|---|---------|
| 1    | Wet Cooling        | 1.523   | 0.8695  | 1.75    |
| 2    | MQL Cooling        | 0.8278  | 0.6210  | 1.33    |

The percentage increase of G-ratio between the wet and MQL cooling conditions was observed to be 24 percent. This was due to the active participation of grains, which confirmed that the material removal rate and wheel wear were higher in wet cooling condition.

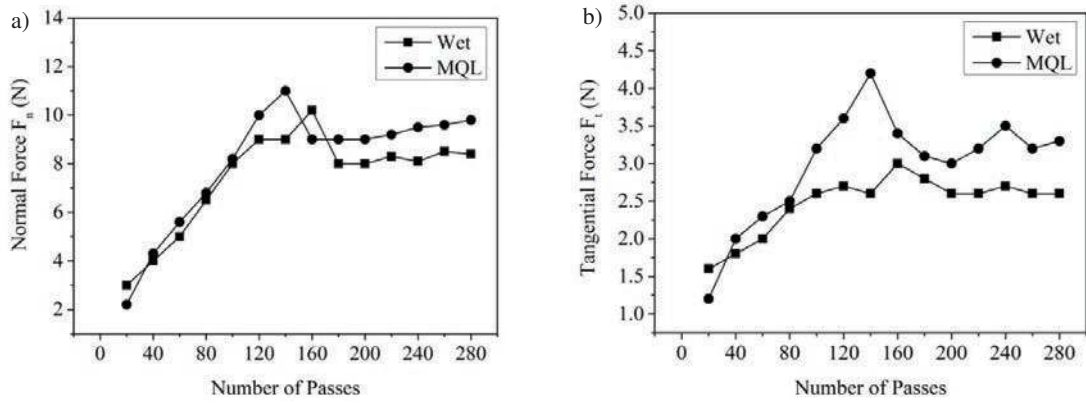


Fig. 5. (a) Variation of normal force with respect to the number of grinding passes, (b) Variation of tangential force with respect to the number of grinding passes

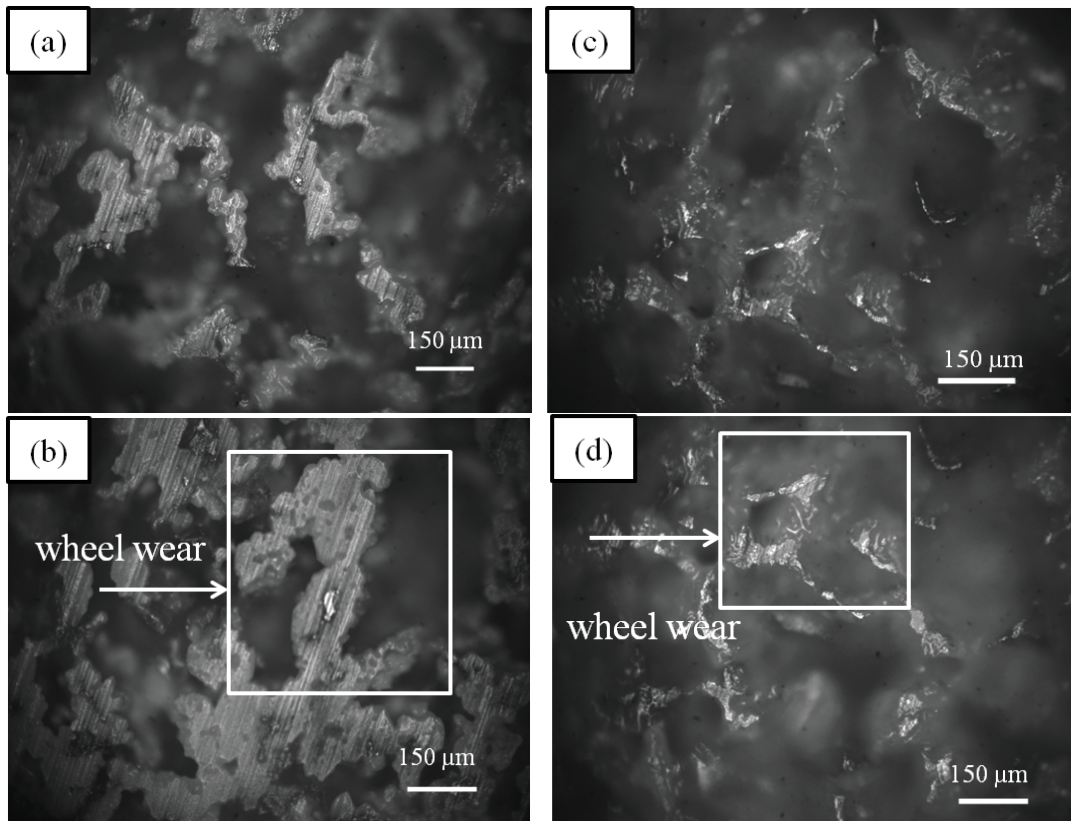


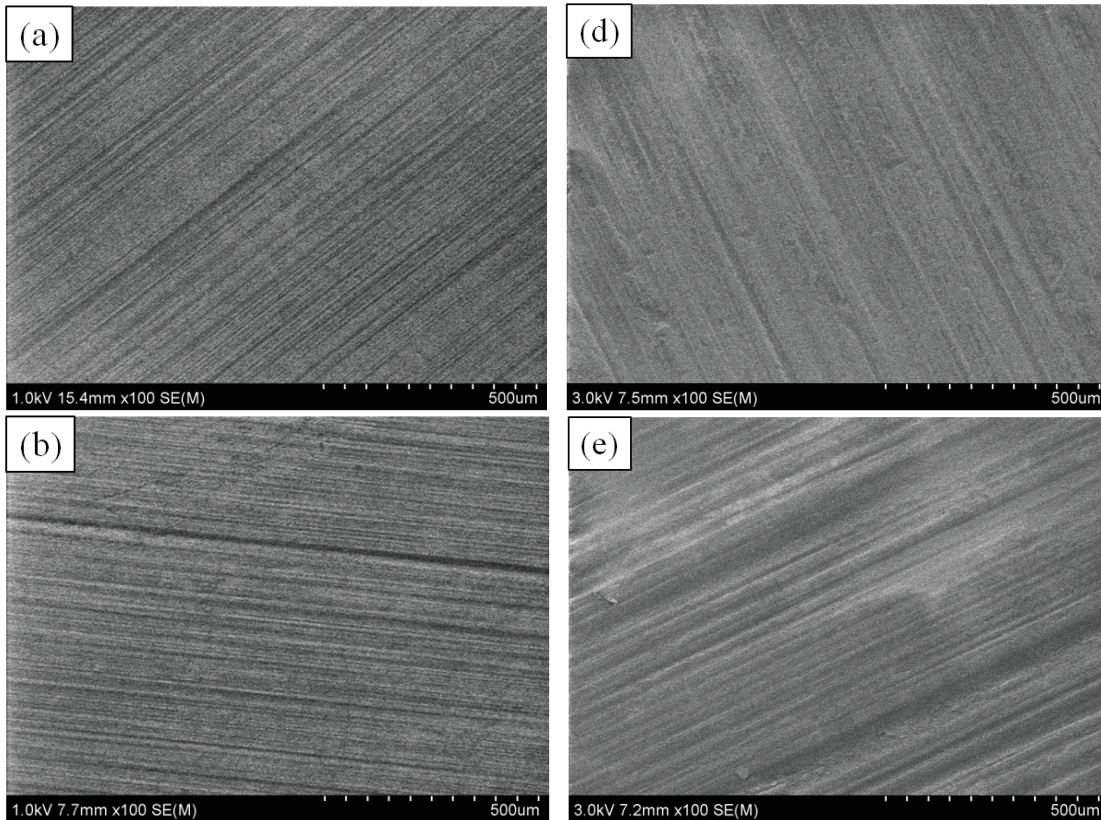
Fig. 6. Optical images of grinding wheel (a) Wet condition - After 120 passes, (b) Wet condition - After 240 passes, (c) MQL condition - After 120 passes, (d) MQL condition - After 240 passes.

The optical images of grinding wheel after 160 passes for both wet and MQL cooling condition are shown in Fig 6. The images obtained from the wet cooling condition showed a clear view of wheel wear, which confirmed the active

grain participation. During MQL grinding condition, the images showed that the grains were not properly involved in the cutting action due to the boundary layer formation.

### 3.5 Ground Surface

The surfaces of both the wet and MQL ground components were viewed with the help of SEM images. A smooth surface with multiple grinding marks was clearly obtained from the wet cooling condition, where the material removal took place easily accompanied with the coolant. Practically, the grinding process was dominated by cutting action, which enhanced the material removal rate by the active participation of grains and resulted in high wheel wear. The ground components obtained from the MQL grinding process showed an irregular pattern of grinding marks, which indicated that the grains were not properly involved in cutting action due to the interlayer formation between the wheel and the surface. Probably the chips were not completely removed from the pores of the grinding wheel, which caused the damages to the surface. The surface morphology of ground samples for both the wet and MQL cooling conditions is shown in Fig 7.



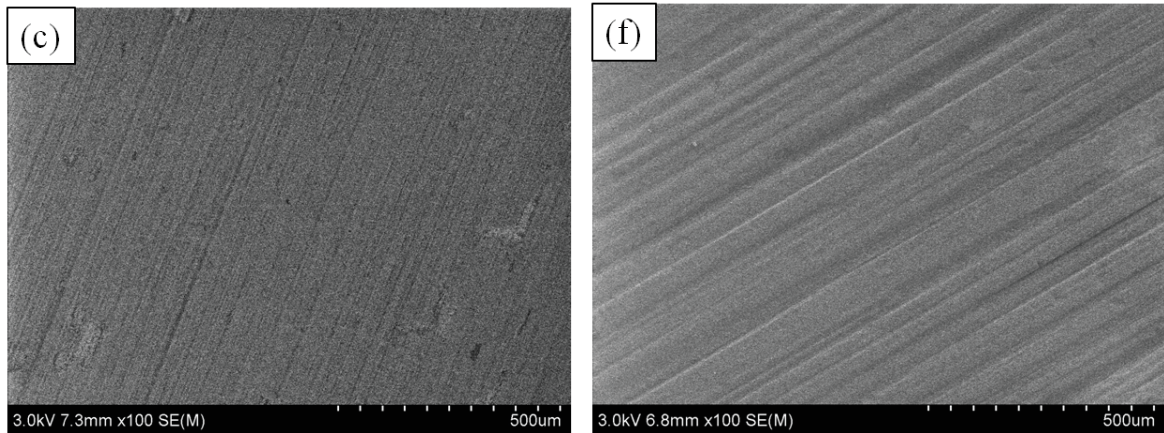


Fig. 7. Surface morphology of ground samples for grinding condition of 20  $\mu\text{m}$  radial depth of cut and 6 m/min feed rate. Wet cooling condition (a) 22 m/s, (b) 32 m/s and (c) 42 m/s, MQL cooling condition (d) 22 m/s, (e) 32 m/s and (f) 42 m/s.

#### 4. Conclusion

The dense vitreous bond of silicon carbide wheel was used to grind the pre-sintered form of Y-TZP under both the wet and MQL cooling conditions. The grindability of pre-sintered zirconia was studied through the analysis of force ratio, specific energy, surface finish, G-ratio and ground surface.

- The grinding forces were less for the MQL cooling condition compared to the wet condition, because of the interlayer formation between the wheel and the work piece surface. The thicker oil film further reduced the friction at the contact zone.
- During the MQL cooling condition, the specific energy required to remove the material became less compared to the wet cooling condition. This was due to the reduction in heat generation and friction.
- The surface finish obtained from the wet cooling condition showed a better performance compared to the MQL condition. It was recommended to use a compressed jet of air to clean the surface of the grinding wheel after every cycle in MQL cooling condition, which improved the surface finish of the material.
- The evaluated G-ratio was improved for wet cooling condition due to the enhanced material removal process, as compared to the MQL condition.
- As the wheel got worn out heavily due to the active participation of grains in the wet cooling condition, the observed results showed that the wheel wear was more with increase in grinding passes. In MQL cooling condition, the inter layer was formed between the wheel and the surface, it did not allow the grains to participate in cutting action and the supplied oil mist was not sufficient to remove the chips present in the pores, which leads to wheel loading.
- The ground surfaces of wet ground components that were viewed through SEM images showed a clear regular grinding marks, which confirmed that the surface finish was good compared to MQL ground components. This investigation explained the grindability of pre-sintered zirconia with dense vitreous bond silicon carbide wheel under both wet and MQL cooling conditions for biomedical applications.

#### References

- [1] J. Chevalier, What future for zirconia as a biomaterial? *Biomaterials*, 27 (2006) 535-543.
- [2] I. Denry, J.R Kelly, State of the art of zirconia for dental applications. *Dental Materials*, 24 (2008) 299-307.
- [3] G. Kaya, Production and characterization of self-colored dental zirconia blocks. *Ceramics International*, 39 (2013) 511-517.
- [4] C. Monaco, A. Tucci, L. Esposito, R. Scotti, Microstructural changes produced by abrading Y-TZP in presintered and sintered conditions. *Journal of dentistry*, 41 (2013) 121-126.
- [5] V. E. Annamalai, T. Sornakumar, C. V. Gokularathnam, R. Krishnamurthy, Efficient grinding of Ce-TZP with SiC wheels. *Journal of the European Ceramic Society*, 11 (1993) 463-469.

- [6] A. J. Shih, T. M. Yonushonis, High infeed rate method for grinding ceramic workpiece with silicon carbide grinding wheels. (2001) US Patent Number 6,220,933.
- [7] J. S. Albert, O. S. Ronald, C. C. Adam, M. Y. Thomas, J. G. Darryl, et al., Cost-effective grinding of zirconia using the dense vitreous bond silicon carbide wheel. *Journal of Manufacturing Science and Engineering*, 125(2) (2003) 297-303.
- [8] L. M. Xua, Bin Shenb, J. S. Albert, Vitreous bond silicon carbide wheel for grinding of silicon nitride. *International Journal of Machine Tools & Manufacture*, 46 (2006) 631-639.
- [9] Mutlu Özcan., Cláudia Ângela Maziero Volpato, Márcio Celso Fredel, Artificial aging of zirconium dioxide: an evaluation of current knowledge and clinical relevance. *Current Oral Health Reports*, 3 (2016) 193-197.
- [10] G. K.R. Pereira, T. Silvestri, R. Camargo, M. P. Rippe, M. Amaral, et al., Mechanical behavior of a Y-TZP ceramic for monolithic restorations: effect of grinding and low-temperature aging. *Materials Science and Engineering C*, 63 (2016) 70-77.
- [11] C. Schröder, A. Renz, C. Koplín, A. Kailer, Assessment of low-temperature degradation of Y-TZP ceramics based on Raman-spectroscopic analysis and hardness indentation. *Journal of the European Ceramic Society*, 34 (2014) 4311-4319.
- [12] T. Tawakoli, M. J. Hadad, M. H. Sadeghi, A. Daneshi, S. Stockert A. Rasifard, An experimental investigation of the effects of work piece and grinding parameters on minimum quantity lubrication - MQL grinding. *International Journal of Machine Tools & Manufacture*, 49 (2009) 924-932.
- [13] D. D. J. Oliveira, L. G. Guermãndi, E. C. Bianchi, A. E. Diniz, P. R. de Aguiar, R. C. Canarim, Improving minimum quantity lubrication in CBN grinding using compressed air wheel cleaning. *Journal of Materials Processing Technology*, 212 (2012) 2559-2568.
- [14] M. Emami, M. H. Sadeghi, A. A. D. Sarhan, Minimum Quantity Lubrication in grinding process of zirconia ( $ZrO_2$ ) engineering ceramic. *International Journal of Mining, Metallurgy & Mechanical Engineering*, 1 (2013) 187-190.
- [15] K. Subramanian, A. Jain, R. Vairamuthu, M. Brij Bhushan, Tribology as an enabler for innovation in surface generation processes. *Proceedings of the ASME 2015 International Mechanical Engineering Congress and Exposition IMECE*. 15 (2015) 1–11.